ADVANCES IN SEMICONDUCTOR SUPERLATTICES, QUANTUM WELLS AND HETEROSTRUCTURES

L. Esaki

JOURNAL DE PHYSIQUE
Colloque C5, supplément au n°4, Tome 45, avril 1984

ADVANCES IN SEMICONDUCTOR SUPERLATTICES, QUANTUM WELLS AND HETEROSTRUCTURES

L. Esaki

IBM T.J. Watson Research Center, Yorktown Heights, New York 10598, U.S.A.

Résumé – Un certain nombre de développements intéressants concernant les études effectuées sur les super-réseaux semiconducteurs, les puits quantiques et les hétérojonctions sont présentés sous forme de revue à partir d'une description des résultats importants obtenus entre 1969 et 1974. Cette présentation est scindée en trois parties qui traitent respectivement de GaAs-GaAlAs, de InAs-GaSb et d'autres systèmes. Ces trois catégories correspondent au matériau support utilisé. Parmi les sujets abordés, on trouve les phénomènes de transport dans les super-réseaux, l'absorption optique, les lasers, les photocourants, la luminescence, la diffusion Raman, l'effet magnéto-quantique, la modulation du dopage, l'effet Hall quantique, les états d'impuretés et les excitons dans les puits quantiques, la magnéto-absorption dans l'infra-rouge lointain, la résonance cyclotronique, les super-réseaux polytypes et les puits quantiques à l'arséniure d'indium.

Abstract - Following a description of highlights during the early period (1969-1974), a series of interesting developments and subsequent ramifications in the studies on semiconductor superlattices, quantum wells and heterostructures, are reviewed by dividing them into thee categories: GaAs-GaAlAs, InAs-GaSb and other systems, according to the host materials. The subjects include superlattice transport, optical absorption, lasers, photocurrent, luminescence, Raman scattering, magnetoquantum effect, modulation doping, quantized Hall effect, impurity states and excitons in quantum wells, far-infrared magneto-absorption, cyclotron resonance, polytype superlattices and InAs quantum wells.

I. INTRODUCTION

Interfaces, as witnessed by the long history of rectifying metal-semiconductor contacts, have been playing a most significant role in many semiconductor devices, including metal-oxide-semiconductor FETs. Research on interfaces and their related effects has been active since the 1930's when the quantum mechanical approach was established. More recently, hetero-epitaxial interfaces between two dissimilar and yet closely lattice-matched semiconductors are of great interest, because technological advances in epitaxy such as the availability of MBE or MOCVD facilitated the dramatic reduction in extrinsic interface defects detrimental to the electron mobility and other device parameters. In such heterostructures, since experimental reality is approaching theoretical models and assumptions, detailed analyses and precise predictions are unprecedentedly made possible.

In this context, in 1969-1970, Esaki and Tsu[1,2] proposed a synthesized semiconductor superlattice of a one-dimensional periodic structure of alternating ultrathin layers with its period less than the electron mean free path. In the insert of Fig. 1, such a superlattice structure is illustrated. The idea of the superlattice occurred to us when examining the possible observation of resonant tunneling through double and multiple barriers. Such resonant tunneling arises from the interaction of de Broglie electron waves with potential barriers.[3] The electron mean free path, an important parameter for the observation of quantum effects, depends heavily on crystal quality and also on temperatures, the effective mass, etc. If characteristic dimensions such as a superlattice period are reduced to less than the electron mean free path, the entire electron system enters into a quantum regime with the assumption of the presence of ideal interfaces, as schematically illustrated in Fig. 1. Our effort for the semiconductor superlattice is viewed as a search for novel phenomena in such a regime.

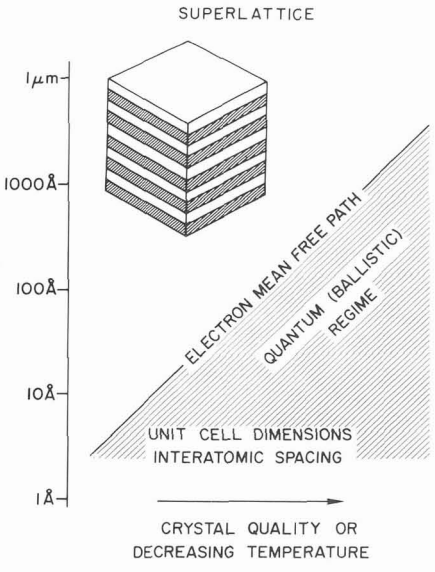

Fig. 1 Schematic illustration of a quantum regime (hatched). A superlattice structure is shown in the insert.

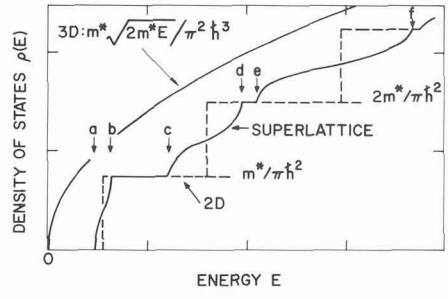

Fig. 3 The comparison of the density of states for the three-dimensional and two-demensional electron systems with that of a superlattice.

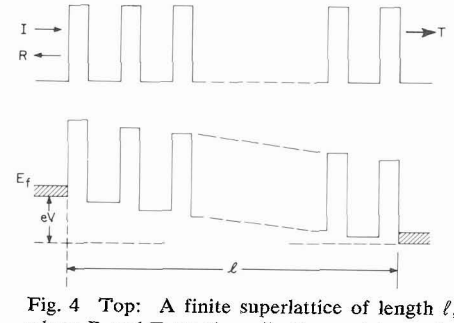

Fig. 4 Top: A finite superlattice of length ℓ, where R and T are the reflection and transmission amplitudes. Bottom: The potential profile with the application of a voltage V.

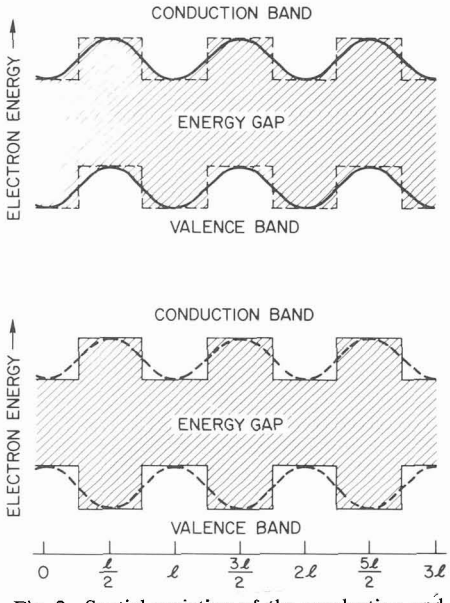

Fig. 2 Spatial variation of the conduction and valence bandedges in two types of superlattices: top, doping superlattice of alternating n-type and p-type layers; bottom, compositional superlattice with alternation of crystal composition.

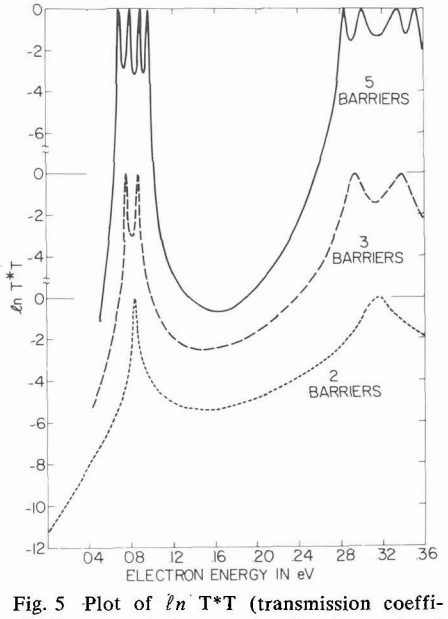

Fig. 5 Plot of ℓn T*T (transmission coefficient) versus electron energy showing peaks at the energies of the bound states in the potential wells. The curves labelled "2 barriers," "3 barriers" and "5 barriers" correspond to one, two and four wells, respectively.

In this review, we first describe the pioneering work during the early period (1969-1974) which is believed to have inspired subsequent explorations on quantum wells and other heterostructures. Our early efforts[4] focussed on transport properties in the direction of the one-dimensional periodic potential. Later, however, it was noticed that optical studies such as absorption, luminescence, lasers, magneto-absorption and inelastic light scattering, and magneto-quantum transport of the two-dimensional electron gas systems in the layer plane prevailed. Such expanded activities resulted in new discoveries and inventions, leading to further proliferation of heterostructures in general. Some of the most significant developments in recent years will be summarized in Chapter III.

II. EARLY PERIOD

1) Proposal of a Semiconductor Superlattice

Esaki and Tsu[1,2] envisioned two types of synthesized superlattices: doping and compositional, as shown in the top and bottom of Fig. 2, respectively, where, in either case, a superlattice potential was introduced by a periodic variation of impurities or composition during epitaxial growth. It was theoretically shown that such a synthesized structure possesses unusual electronic properties not seen in the host semiconductors, arising from predetermined quantum states of two-dimensional character.

The introduction of the superlattice potential clearly perturbs the band structure of the host materials: The degree of such perturbation depends on its amplitude and periodicity. Since the superlattice period ℓ is usually much greater than the original lattice constant, the Brillouin zone is divided into a series of minizones, giving rise to narrow allowed subbands, E_1, E_2..., separated by forbidden regions, in a highly perturbed energy-wave vector relationship for conduction electrons. Figure 3 shows the density of states $\rho(E)$ for electrons in a superlattice in the energy range including the first three subbands: E_1 between a and b, E_2 between c and d and E_3 between e and f (indicated by arrows in the figure), in comparison with the parabolic curve for the three-dimensional electron system and the staircase-like density of states for the two-dimensional system. The analyses on the dynamics of conduction electrons in such narrow subbands predicted the occurrence of a differential negative resistance in the transport characteristic of the superlattice direction.

Although the situation is analogous to the Kronig-Penney band model,[5] it is seen here that the familiar properties are observed in a new domain of physical scale. In an extreme case, where quantum wells are sufficiently apart from each other, allowed bands become discrete states, and then electrons are completely two-dimensional in which the density of states is illustrated by the dashed line in Fig. 3.

It is worthwhile mentioning that, in 1974, Gnutzmann et al.[6] pointed out an interesting possibility; namely, the occurrence of a direct-gap superlattice made of indirect-gap host materials, because of Brillouin-zone folding as a result of the introduction of the new superlattice periodicity. The idea may suggest the synthesis of new optical materials.

2) Experimental Efforts

In 1970, Esaki et al.[7] reported the first experimental result on a superlattice synthesized by the CVD technique. The structure was obtained by a periodic variation of the phosphorus content, x, in the $GaAs_{1-x}P_x$ system. The period was made as thin as 200Å with x varying from 0-0.1 to 0.5. Although the superlattice formation was clearly demonstrated by electron microscopy, X-ray diffraction and cathode luminescence, transport measurements failed to show any predicted quantum effect. In this system, a relatively large lattice-mismatch, 1.8%, between GaAs and $GaAs_{0.5}P_{0.5}$ inevitably generates a strain at the interfaces.

It was recognized at the beginning that, while the structure was undoubtedly of considerable theoretical interest, the formation of such a refined layer-structure would be a formidable task. Nevertheless, the proposal of a semiconductor superlattice inspired a number of material scientists to produce alternating layers of lattice-matched GaAs and $Ga_{1-x}Al_xAs$ with the MBE and LPE techniques. In 1972, we established a MBE system particularly designed for the superlattice structure, which led to the successful growth of a GaAs-GaAlAs superlattice.[8] Esaki et al.[9] found that this superlattice exhibited a negative resistance in its transport properties, which was, for the first time, interpreted on the basis of the predicted quantum effect. The superlattice structure was grown between two doped GaAs layers. The samples were evaluated with various techniques including HEED, He-ion backscattering, and Raman scattering. The compositional profile of such a structure was directly verified by the simultaneous use of ion sputter-etching of the sample surface and Auger electron spectroscopy.[10]

3) Multibarrier Tunneling

In 1973, Tsu and Esaki[11] computed the transport properties from the tunneling point of view, leading to the derivation of I-V curves. The superlattice band model previously presented, assumes an infinite periodic structure. In reality, however, not only a finite number of periods is prepared with alternating epitaxy, but also the electron mean free path is limited. In addition, two terminal electrodes for transport measurements, which create interfaces between the superlattice and such electrodes, are unavoidable. The potential profile of the realistic system is schematically illustrated in Fig. 4, where the top and the bottom are an n-period superlattice of a finite length ℓ used for calculations of the reflection R and transmission T amplitudes, and the tunnel current J as a function of applied voltage V, respectively. Incidentally, one will notice in this system that one-dimensional localization results from the fact that the two terminal electrodes serve as reservoirs which randamize the phase of electron waves.

In Fig. 5, ℓnT*T is plotted as a function of electron energy for a double, a triple and a quintuple barrier structure, showing unity transmissivity at resonant energies. Note that the resonant energies for the triple-barrier (double-well) case are split into doublets, and those for the quintuple barrier (quadruple-well) case are split into quadruplets. In the double-well case, each single-well quantum state is split into a symmetric and an antisymmetric combination. This is extended to n wells. In the large n limit, a band-like condition is ultimately achieved, which corresponds to the superlattice band model. We believe that this multibarrier tunneling model provided a useful insight into the transport mechanism and laid the foundation for the following experimental investigations.

4) Search for Quantum States

In early 1974, Chang et al.[12] observed resonant tunneling in double barriers, and subsequently Esaki et al.[13] measured quantum transport properties for a superlattice having a tight-binding potential. The I-V and dI/dV-V characteristics are shown in Fig. 6 for a double barrier with a well of 50Å and two barriers of 80Å made of $Ga_{0.3}Al_{0.7}As$. The schematic energy diagram is shown in the inset where the first two quantized levels are indicated. The resonance, in this case, is achieved under applied voltages by aligning the Fermi level of the electrode with the bound quantum states. The current should show peaks at voltages equal to twice the energies of the bound quantum states referred to the original conduction band edge in the well. The situation is shown as (a) and (c) in the energy diagrams and is also marked correspondingly in the experimental curves in Fig. 6, where two sets of singularities are clearly visible. The broadness of the signularities comes mainly from the fluctuations in both thicknesses and potentials that may exist in the formation of the double-barrier structure. As large number of double barriers were made with three different well widths, 40, 50, and 65Å. Although there is some understandable spread, measured values for the quantized levels have been verified to coincide with the calculated ones. This agreement undoubtedly has confirmed the observation of resonant tunneling and, consequently, the energies of the bound quantum states.

These experiments probably constitute the first clear observation of quantum states in both single and multiple potential wells. The impact of the achievement of superlattices or multibarrier structures is many-fold. The elegance of the one-dimensional quantum physics, which had long remained a textbook exercise, could now, for the first time, be practiced in a laboratory (Do-It-Yourself Quantum Mechanics!). It should be emphasized that such an achievement would not have been accomplished without the key contribution of material preparation techniques.

5) Interfaces

For analyses of superlattice structures, the high-angle as well as the low-angle X-ray scattering data provided relevant information[14] including the accurate determination of the superlattice period as well as the elastic strain present in the lattice. The measured elastic strain agreed with the value computed theoretically on the assumption that the strain is not relieved by misfit dislocations at the interfaces. Some deviations from the ideal structure are also evident from the observation. At the GaAs-AlAs interface there will be mixed layers even if there is no diffusion because at the instant one beam is shut off and the other beam switched on, the surface will, in general, have a partial layer with an atomic step in it. This causes a rounding of the edges of the composition profile at the interface and produces incommensurate superlattice periods. Recently, Weisbuch et al.[15] reported some estimates of interface roughness for GaAs-GaAlAs multi-quantum well structures, analyzed from broadening of luminescence linewidths, which suggested the presence of the island-like structure with a one monolayer height and a lateral size of 300Å or more.

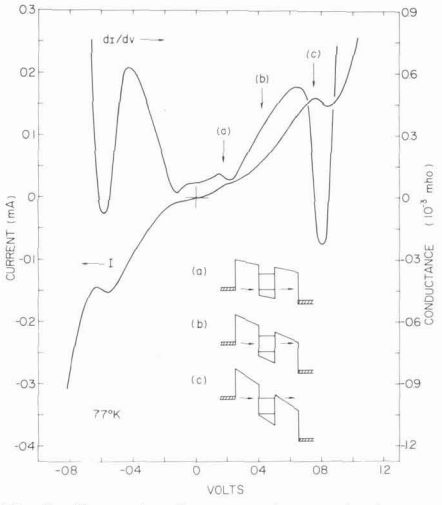

Fig. 6 Current-voltage and conductance-voltage characteristics of a double-barrier structure. Conditions at resonance (a) (c) and off-resonance (b) are indicated.

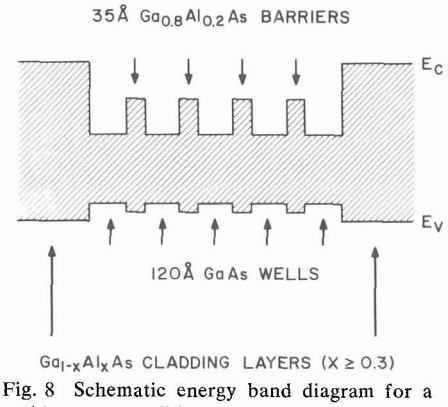

Fig. 8 Schematic energy band diagram for a multiquantum-well laser.

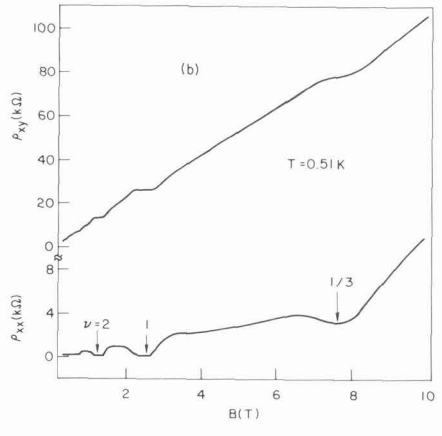

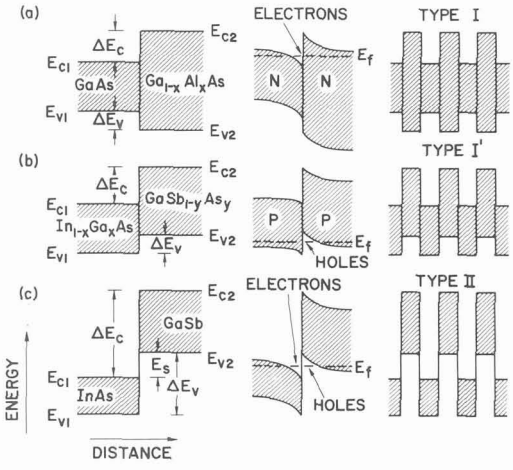

Fig. 7 The relationship of bandedge energies at the heterojunction interfaces for (a) GaAs-$Ga_{1-x}Al_xAs$, (b) $In_{1-x}Ga_xAs$-$GaSb_{1-y}As_y$ and (c) InAs-GaSb (left) and the energy band diagrams of their respective superlattices or multiquantum wells (right). The band-bending and carrier confinement at the heterojunction interfaces (middle).

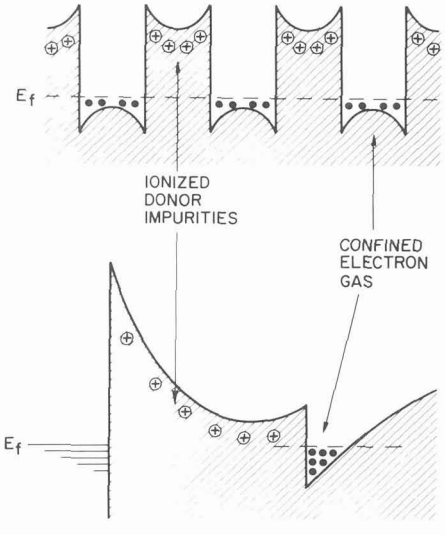

Fig. 9 Modulation doping for a superlattice (top) and a heterostructure with an attached Schottky junction (bottom).

Fig. 10 Magnetoresistance ρ_{xx} and Hall resistance ρ_{xy} as a function of magnetic field at 0.51K for a heterojunction with an electron concentration of 0.6 x $10^{11}cm^{-2}$.

One should realize that the superlattice proposal was made on a rather optimistic presupposition of a "clean" and yet atomically smooth interface which provides only an abrupt potential step with little undesirable localized states. Recently, considerable efforts have been made to understand the electronic structure at interfaces[16] or heterojunctions.[17,18] Even in an ideal situation, the discontinuity at the interface provides formidable tasks in theoretical handling: Propagating and evanescent Bloch waves should be matched across the interface, satisfying continuity conditions on the envelope wave functions.[19,20] The interface chemical bonds differing from the bulk may give rise to localized states in addition to bond-relaxation in some circumstances.

In reality, however, the presence of possible misfit dislocations and other defect-complexes, as well as roughness or disorder at the interface may not be completely avoidable even with most advanced techniques. Indeed, the early experimental results described in this chapter suffered considerably from such departures from an idealized model on which simple theories are based. The extrinsic effects due to localized states around defect sites near the interface should be distinguished from the intrinsic properties arising from the discontinuities of the wave functions. In favorable systems such as GaAs-GaAlAs, the intrinsic localized states are virtually nonexistent in the energy range in which we are interested.

III. IMPORTANT DEVELOPMENTS

1) Remarks

In this review, we will try to describe some of the important developments by categorizing them according to host materials used: GaAs-$Ga_{1-x}Al_xAs$, InAs-GaSb(-AlSb), and other superlattice systems. Such categorization, however, often encounters difficulties because similar studies extend over a variety of materials; the same experimental techniques and theoretical methods can be easily applied to different systems. Nevertheless, most significant studies from scientific as well as technological aspects have been carried out with GaAs-$Ga_{1-x}Al_xAs$ and InAs-GaSb systems. In Fig. 7, three typical examples for the relationship of bandedge energies at heterojunctions (left) and their respective superlattices or multiquantum-wells (right) are shown together with corresponding band-bending and carrier confinement at the interface (middle). The conduction band discontinuity ΔE_c is equal to the difference in the electron affinities of the two semiconductors. In case (c), the band-bending and electron and hole confinements occur, as indicated, regardless of the polarity of employed semiconductors, whereas, in cases (a) and (b), those depend on the semiconductor polarity (N or P).

As seen in Fig. 7, in the GaAs-$Ga_{1-x}As_xAs$ system, the total difference in the energy gaps is shared by potential steps ΔE_c and ΔE_v, while the InAs-GaSb system exhibits a rather unusual bandedge relationship; namely, the conduction bandedge of InAs, E_{c1}, is lower than the valence bandedge of GaSb, E_{v2}, by E_g. The superlattices made of these three types of semiconductor pairs are identified as type I, type I' and type II, as illustrated from the top to the bottom on the right side. Although a variety of superlattices have been synthesized with many semiconductor pairs, all of them will fall into these three categories.

2) GaAs-GaAlAs

i) Optical Absorption

Dingle et al. observed pronounced structure in the optical absorption spectrum, representing bound states in isolated[21] and coupled quantum wells.[22] For the former, GaAs well widths in the range between 70Å and 500Å were prepared. In low-temperature measurements for such structures, several exciton peaks, associated with different bound-electron and bound-hole states, were resolved. For the latter study, a series of structures, with GaAs well widths in the range between 50Å and 200Å and $Ga_{1-x}Al_xAs$ ($0.19<x<0.27$) barrier widths between 12Å and 18Å, were grown by MBE on GaAs substrates. The spectra at low temperatures clearly indicated the evolution of resonantly split discrete states into the lowest band of a superlattice. These observations demonstrated the great precision of MBE in fabricating thin and uniform layers.

ii) Lasers

van der Ziel et al.[23] observed optically pumped laser oscillation from the above-mentioned quantum-well structures at 15K. The laser oscillation occurred at energies which are slightly below the exciton associated with the lowest energy $n = 1$ bound state in GaAs quantum wells (50-500Å thick).

More recently, Tsang[24] succeeded in attaining a threshold current density J_{th} as low as 250A/cm^2 in MBE-grown $Ga_{1-x}Al_xAs$-GaAs laser diodes with a multiquantum-well structure as shown in Fig. 8. This was achieved as a result of utilizing the beneficial effects arising from the two-dimensional density of states of the confined carriers (Fig. 3). It is generally observed that, in mutliquantum-well lasers, the beam width in the direction perpendicular to the junction plane and the temperature dependence of J_{th} are significantly reduced in comparison with the regular double-heterostructure (DH) lasers.

iii) Photocurrent and Luminescence

Tsu et al.[25] made photocurrent measurements in GaAs-GaAlAs superlattices, which enabled them to observe simulataneously quantum states and associated anomalous transport. The spectrum in the photocurrent shows a series of peaks of photon energies corresponding to interband transitions between the subbands.

More recently, Mendez et al.,[26] with a somewhat similar experimental arrangement, observed an electric field-induced quenching of photoluminescence from quantum wells. Six identical GaAs quantum wells (width = 35Å) in GaAlAs medium were formed in the space charge region of the Schottky barrier. With an increasing applied field perpendicular to the quantum wells, the luminescence intensity decreases and becomes completely quenched at an average field of a few tens of kV/cm, (applied voltage = -0.4V). The observation is interpreted as caused by the field, which induces a separation of electrons and holes in the quantum well with the modification of the quantum states in the wells, resulting in luminescence quenching.

iv) Raman Scattering

Manuel et al.[27] reported the observation of enhancement in the Raman cross section for photon energies near electronic resonance in GaAs-$Ga_{1-x}Al_xAs$ superlattices of a variety of configurations. Both the energy positions and the general shape of the resonant curves agree with those derived theoretically based on the two-dimensionality of the quantum states in such superlattices. Polarization studies indicate a major contribution to the scattering from forbidden processes.

Among recent developments in the field have been the introduction of inelastic light scattering as a spectroscopic tool in the investigation of the two-dimensional electron system. The significance of resonant inelastic light scattering was first pointed out by Burstein et al.,[28] claiming that the method yields separate spectra of single particle and collective excitations which will lead to the determination of electronic energy levels in quantum wells as well as Coulomb interactions. Subsequently, Abstreiter et al.[29] and Pinczuk et al.[30] observed light scattering by intersubband single particle excitations, between discrete energy levels, of two-dimensional electrons in GaAs-$Ga_{1-x}Al_xAs$ heterojunctions and quantum wells.

Meanwhile, Colvard et al.[31] reported the observation of Raman scattering from folded acoustic longitudinal phonons in a GaAs(13.6Å)-AlAl(11.4Å) superlattice. The superlattice periodicity is expected to result in Brillouin-zone folding (as previously mentioned) and the appearance of gaps in the phonon spectrum for wave vectors satisfying the Bragg condition. An explanation of the data was given with a simple theory which involves the Kronig-Penney electron model and the phonons in the elastic continuum limit.

v) Magnetoquantum Effects

In 1977, Chang et al.[32] reported the first observation of the oscillatory magnetoresistance (Shubnikov-de Haas effect) in GaAs-$Ga_{1-x}Al_xAs$ superlattices with the current flowing in the plane of the layers. The superlattice provides a unique opportunity to create made-to-order Fermi surfaces by controlling the energy and bandwidth of the subbands which are determined by the barrier and well-thicknesses as well as the barrier height. The observed oscillations manifest the electronic subband structure, which becomes increasingly two-dimensional in character as the bandwidth is narrowed. The detailed analysis of the data indicated a good agreement with the Fermi surfaces calculated on the basis of the superlattice configuration and the electron concentration.

In 1980, Tsui et al.[33] reported the first observation of magnetophonon resonances in the two-dimensional electron system in GaAs-GaAlAs heterojunctions and superlattices. The resonances, detected in the magnetic field dependence of the samples resistance at temperatures between 100 and 180K, result from inelastic scattering of electrons between Landau levels with resonant absorption of GaAs LO phonons under the resonance condition of $N\hbar\omega_c = \hbar\omega_o$ where $\hbar\omega_c$ is the Landau level spacing, ω_o, the phonon frequency and N, an integer. The result showed that, in this system, the electron-phonon interaction with the polar mode of

GaAs is dominant and its strength is consistent with that expected from polar coupling of two-dimensional electrons to the LO phonons of bulk GaAs.

vi) Modulation Doping and High Speed Devices

It is usually the case that free carriers, electrons or holes, in semiconductors are created by doping impurities: donors or acceptors. Thus, carriers inevitably suffer from impurity scattering. There are a few exceptions. Insulated-gate effect devices (MOSFET) are one such example, where electrons or holes are induced by applied gate voltages. InAs-GaSb superlattices may be another example where electrons and holes are produced solely by the unique bandedge relationship, as described later.

Now, in superlattices, it is possible to spatially separate carriers and their parent impurity atoms by doping impurities in the regions of the potential hills, as shown in Fig. 9. In the original article,[1] this concept was expressed in the general terms. In 1978, Dingle et al.[34] successfully implemented such a concept in modulation-doped GaAs-GaAlAs superlattices, as illustrated in the top of Fig. 9, achieving electron mobilities which exceed the Brooks-Herring predictions. Modulation doping was performed by synchronizing the silicon (n-dopant) and aluminum fluxes in the MBE, so that the dopant was distributed only in the GaAlAs layers and was absent from the GaAs layer.

In 1980, Mimura et al.[35] and Delagebeaudeuf et al.[36] applied modulation-doped GaAs-GaAlAs heterojunctions to fabricate a new high-speed FET called HEMT (High Electron Mobility Transistor) or TEGFET (Two-Dimensional Electron Gas Field Effect Transistor), of which the energy diagram is shown in the bottom of Fig. 9. The device, if operated at 77K, apparently exhibits a high-speed performance three times superior to that of the conventional GaAs MESFET.

vii) Quantized Hall Effect

In 1980, Klitzing et al.[37] demonstrated an interesting proposition that quantized Hall resistance can be used for precision determination of the fine structure constant α, using two-dimensional electrons in the inversion layer of a Si MOSFET (Metal-Oxide-Semiconductor Field Effect Transistor). Subsequently, Tsui et al.[38] found that, with the modulation-doped GaAs-GaAlAs heterostructures, the pronounced characteristic of the quantized Hall effect can be easily observed, primarily because of their high electron mobilities, which led to the determination of α with a great accuracy such as $\alpha^{-1} = 137.035965(12)(0.089\text{ppm})$.[39]

The quantized Hall effect in the two-dimensional electron system is observable at sufficiently high magnetic fields and low temperatures when there is little overlap in the density of state of neighboring Landau levels; in such a range of magnetic fields as to locate the Fermi level between the Landau levels, the parallel component of resistance ρ_{xx} vanishes and the Hall resistance ρ_{xy} goes through plateaus, as shown in Fig. 10. This surprising result can be understood by the argument that the localized states do not take part in quantum transport. At the plateaus, the Hall resistance is given by $\rho_{xy} = h/e^2 i = \mu_o c/2\alpha i \approx 25813\ \Omega/i$ where i is the number of filled Landau levels, h the Planck's constance, e the electronic charge, μ_o the vacuum permeability, and c the speed of light in vacuum.

Recently, Tsui et al.[40] discovered a striking phenomenon: the existence of an anomalous quantized Hall effect, a Hall plateau in ρ_{xy} and a dip in ρ_{xx}, at a fractional filling factor of 1/3, as seen in Fig. 10, in the extreme quantum limit at temperatures lower than 4.2K. The result shown in Fig. 10 was recently obtained with a very dilute two-dimensional electron gas ($n = 6 \times 10^{10}\text{cm}^{-2}$) in the modulation-doped GaAs-GaAlAs heterostructures by Mendez et al.[41] Notice that the quantum limit (i=1) and a clear minimum corresponding to $\nu=1/3$ are reached at as low as 2.55T and 7.7T, respectively.

Laughlin,[42] as an explanation of such a fractional filling, presented variational ground-state and excited-state wave functions which describe the condensation of a two-dimensional electron gas into a new state of matter, an incompressible quantum fluid. The elementary excitations of this quantum fluid are fractionally charged, and this elegant theory predicts a series of ground states characterized by the variational parameter m (m=3, 5,...), decreasing in density and terminating in a Wigner crystal. More recently Störmer et al.[43] in addition to previously reported structures at filling factors, $\nu=1/3$ and 2/3, observed new structures at $\nu=4/3$, 5/3, 2/5, 3/5, 4/5, and 2/7. The results suggested that fractional quantization of the Hall effect exists in multiple series, each based on the inverse of an odd integer. There exists no full explanation for all of these experimental results at this moment.

viii) Impurity States and Excitons in Quantum Wells

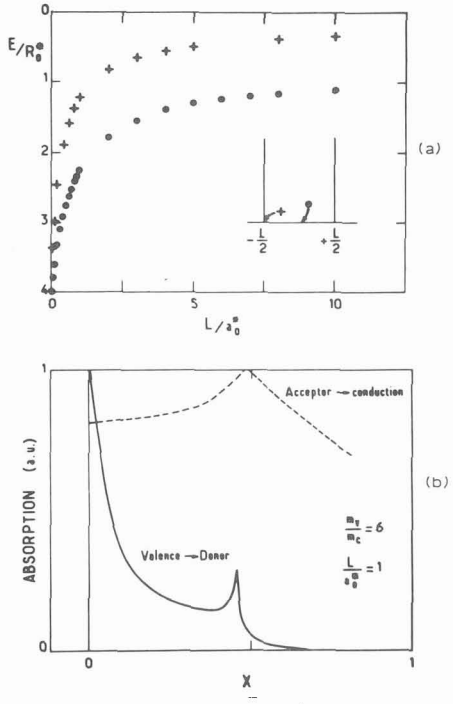

Fig. 11 (a) Binding energy E/R^*_o versus well thickness L/a^*_o, where R^*_o and a^*_o are the three-dimensional effective Rydberg and Bohr radius, respectively. (b) Absorption coefficient versus the dimensionless frequency χ.

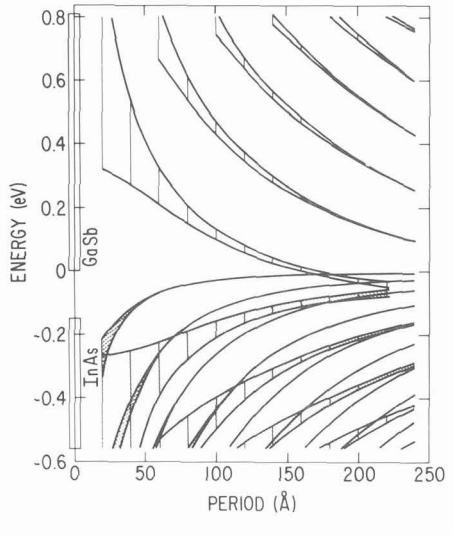

Fig. 13 Calculated subband energies and bandwidths for electrons and light and heavy holes as a function of period, assuming $d_1 = d_2$.

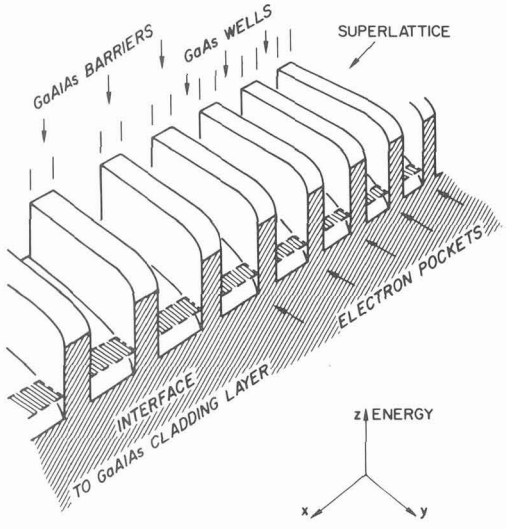

Fig. 12 The quasi-one-dimensional electron system on the surface inversion layer of a superlattice crystal.

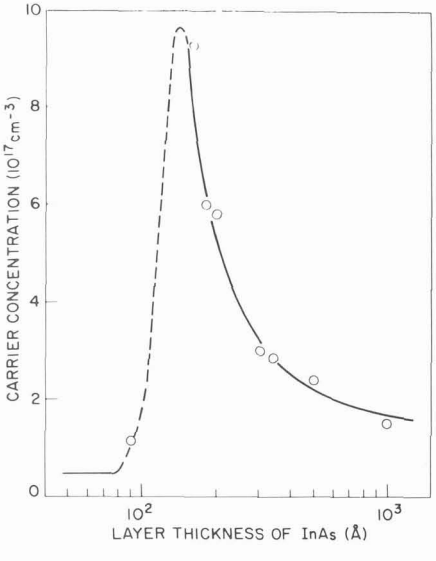

Fig. 14 Carrier concentration vs. layer thickness to demonstrate the semiconductor-semimetal transition.

Bastard[44] performed a variational calculation of the hydrogenic impurity ground states in a quantum well, obtaining the binding energy E as a function of well thickness and of impurity position. Figure 11(a) shows the binding energies in units of R^*_o: the three-dimensional effective Rydberg, at the edge and the center, indicated by crosses and dots, respectively, as a function of the normalized well thickness: L/a^*_o, where a^*_o is the three-dimensional effective Bohr radius. The electron confinement in a potential well lifts the usual ground bround state degeneracy with respect to the impurity position. The dependence of the binding energy on the impurity position leads to the formation of an impurity band. The density of states manifests itself in acceptor → conduction or valence → donor absorption process as two peaks located at the band extrema, as shown in Fig. 11(b), in which the dimensionless frequency χ is given by $\hbar\omega = E_g - E_i^{max} + \chi E_i^{max}$ where E_i refers to donor or acceptor binding energy. Photoluminescence from GaAs quantum wells measured by Miller et al.[45] apparently confirmed Bastard's prediction. Bastard et al.[46] derived the exciton binding energy in quantum wells with variation calculations. Similar calculations were reported by Green et al.[47]

ix) Avalanche Photodiodes with Heterostructures

Superlattices or heterostructures have been exploited to obtain improved avalanche photodiodes. As is known, a large difference in the ionization rates for electrons and holes, α and β, respectively, is desirable for a low noise performance. Unfortunately, most III-V semiconductors have α nearly equal to β Therefore, Chin et al.[48] proposed increasing α/β by using a GaAs-GaAlAs superlattice structure. In this structure, since the conduction bandedge discontinuity ΔE_c is considerably large than the valence bandedge discontinuity ΔE_v, the ionization rate for electrons will be enhanced, but not for holes, thus resulting in an artificial increase of α/β. Capasso et al.[49], indeed, obtained an increased α/β of 10 with a p-i-n structure consisting of 50 alternating 450Å GaAs and 550Å $Ga_{0.55}Al_{0.45}As$ layers. In addition, with the application of band-gap engineering such as graded gap or periodic structures, a number of new photodiodes or photomultipliers have been explored,[50] including channeling avalenche detectors[51] which spatially separate electrons and holes.

x) Attempts for One-Dimensionality

The introduction of a superlattice potential facilitates the reduction of the dimensionality of carriers from three to two at the lower limit in the case of a series of quantum wells. On the other hand, the electrons on the surface inversion layers, as seen in Si MOSFETs, always constitute a two-dimensional gas. Thus, the electron system on the surface inversion layer of a superlattice crystal, as schematically illustrated in Fig. 12, will exhibit the dimensionality between one and two, depending upon the superlattice potential profile. It is assumed here that, using a superlattice being p-type or having no carriers, surface electrons are generated either by an external field or by modulation-doping from a cladding GaAlAs layer (not shown in the figure). If the GaAlAs barriers in the superlattice are sufficiently thick so that wave functions in the electron pockets on the surface have no overlap, then a confined one-dimensional electron gas will be obtained.

Sakaki[52] proposed a V-grooved MOSFET of a one-dimensional electron gas with a single quantum well, virtually similar to that shown in Figure 15, suggesting extremely high electron mobilities on the basis of the scattering probability from Coulomb potential. Petroff et al.[53] attempted the realization of one-dimensional carriers confining structure with MBE-grown GaAs and GaAlAs layers.

3) InAs-GaSb(-AlSb)

i) Theoretical Treatments

In 1976, in search for an alternative to the GaAs-AlAs system, in which the introduction of the superlattice periodicity will give a greater modification to the electronic band structure of the host materials, the InAs-GaSb system appeared as a good candidate because of its unique bandedge relationship at the interface, as shown in Fig. 7. Sakaki et al.[54] confirmed such a relationship with the observation of an unusual nonrectifying characteristic in the p-n junctions made of n-InAs and p-GaSb, which was the direct consequence of "interpenetration" between the GaSb valence band and the InAs conduction band. At the interface, shown in the center at the bottom of Fig. 7, electrons which "flood" from the GaAs valence band to the InAs conduction band, leaving holes behind, produce a strong dipole layer consisting of the two-dimensional electron and hole gases.

First, Sai-Halasz et al.[55] made a one-dimensional calculation for the InAs-GaSb superlattices, treating each host material in Kane's two-band framework. The GaAs-AlAs superlattices, on the other hand, can be adequately treat in one-band approaches. In the InAs-GaSb superlattices, although potential wells for electrons and holes are located in the different semiconductors, quantized levels in the electron wells will be

very close in energy to those in the hole wells. Thus, in such cases, there exists a strong interaction between them.

Next a band calculation was performed with the linear-combination-atomic-orbitals (LCAO) method[56] handling a large size of the primitive cell and ignoring charge redistribution at the interface. The calculated subband structure is strongly dependent upon the period. Figure 13 shows calculated subband energies and bandwidths for electrons and light and heavy holes as a function of period, together with the energy gaps of GaSb and InAs in the left, assuming $d_1 = d_2$, where the semiconducting energy gap is determined by the energy difference between the ground electron and heavy hole subbands. This gap decreases with increase in the period, becoming zero at 170Å, as seen in the figure, corresponding to a semiconductor-to-semimetal transition. This indicates that, by a choice of the period, it is possible to synthesize a tailor-made narrow gap semiconductor or a semimetal with an electronic band structure which bears little resemblance to that of the host semiconductors. Once the system becomes semimetallic with increase in the period, the charge redistribution at the interface will give rise to severe band-bending.

ii) Optical Absorption and Luminescence

Optical absorption measurements[57] were made on InAs-GaSb superlattices with periods ranging between 30 and 60Å which are in the semiconductor regime as indicated in Fig. 13. From measurements of the absorption coefficient α as a function of the photon energy, it is seen that the rise in α is rather weak in comparison with what it would ordinarily be at the bandedge of normal semiconductors, as theoretically expected. The measured absorption edges agree with the calculated energy gaps of the superlattices of various configurations, establishing that the conduction bandedge of InAs lies approximately 0.15eV below the valence bandedge of GaSb.

Recently, Voisin et al.[58] observed luminescence from the similar semiconducting InAs-GaSb superlattices. It was found that, in addition to radiative recombination between the electron and hole ground subbands, the luminescence spectra exhibit a low-energy tail which is believed to arise from impurities and interface defects.

iii) Semiconductor-Semimetal Transitions and Shubnikov-de Haas Oscillations

In order to verify the critical layer thickness[59] for the predicted semiconductor-semimetal transition, a number of InAs-GaSb superlattices with a variety of periods were grown on (100)GaSb substrates whose carriers largely freeze out at low temperatures. The measured electron concentrations at 4.2K were plotted as a function of InAs layer thickness, as shown in Fig. 14. It is evident that the electron concentration exhibits a sudden increase of an order-of-magnitude in the neighborhood of 100Å. This increase indicates the onset of electron transfer from GaSb to InAs, namely, the transition from the semiconducting state to the semimetallic state. The observation is in good agreement with the theoretical prediction, presented in Fig. 13, giving a critical layer thickness for this transition of 85Å, when the energy difference between the GaSb valence bandedge and the InAs conduction bandedge is 0.15eV at the interface. Since this increase in the electron concentration is not due to doping of impurities, mobilities beyond $10^4 cm/V \cdot s$ at 4.2K can be achieved, much higher than bulk InAs with comparable electron concentrations, somehow similar to the modulation-doping.

The subband energy diagrams of two semimetallic superlattices: thin (top) and thick (bottom) are illustrated in Fig. 15, where it is clear that, as the layer thickness is widened, the band bending increases and more than one subband may become involved. As seen in Fig. 14, after reaching a peak, the carrier concentration decreases with increase in thickness and becomes saturated as the superlattice approaches the limit whereby it can be considered as a series of isolated heterojunctions. In this limit, most electronic conduction is taking place at heterojunction interfaces where electrons and holes are accumulated in a two-dimensional fashion.

Chang et al.[60] made extensive Shubnikov-de Haas experiments on superlattice samples covering the entire semimetallic regime from the onset of the semiconductor-semimetal transition to the heterojunction limit, providing a direct measure of the electron density and the Fermi energy.

iv) Far-Infrared Magneto-Absorption and Cyclotron Resonance

Far-infrared magneto-absorption experiments[61,62] were performed at 1.6K for semimetallic 120-80Å, 200-100Å and 1000-1000Å superlattices with radiation near normal incidence to the layers. The transmission signal exhibits oscillations with increase in magnetic field. Figure 16 gives, as a function of the magnetic field B, the infrared energy positions of the transmission minima from such oscillations for the 120-80Å superlattice. The data indicate that the energies at which absorption maxima occur are directly proportional to B and

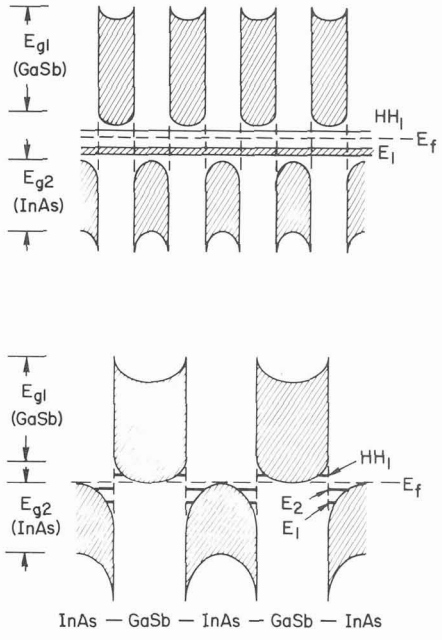

Fig. 15 Schematic illustration of potential-energy profiles for two semimetallic superlattices: thin (top) and thick (bottom) layers, where E_1 and E_2, and HH_1 are the quantized states for electrons and heavy holes, respectively.

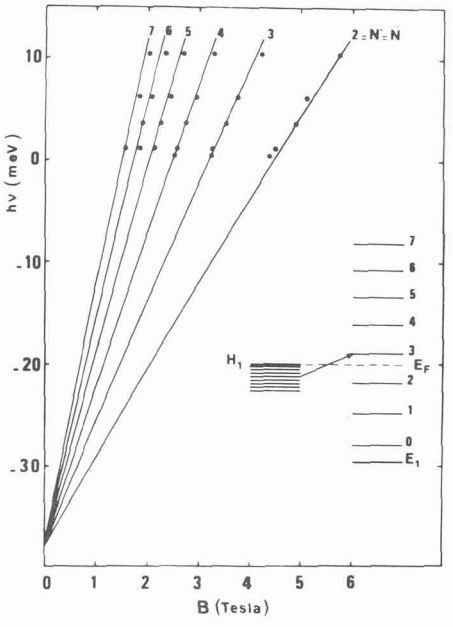

Fig. 16 Magneto-absorption energies vs. B. The inset shows the Landau levels of E_1 and H_1 to illustrate interband transitions.

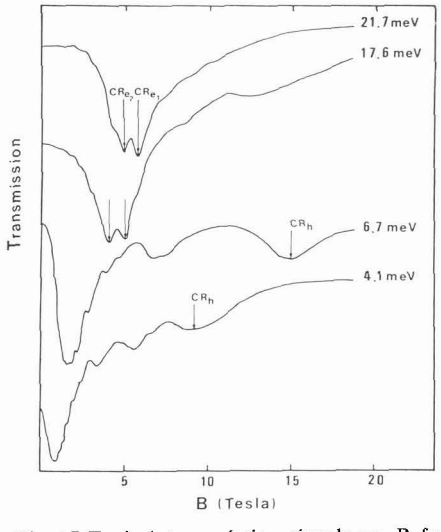

Fig. 17 Typical transmission signals vs. B for different infrared photon energies.

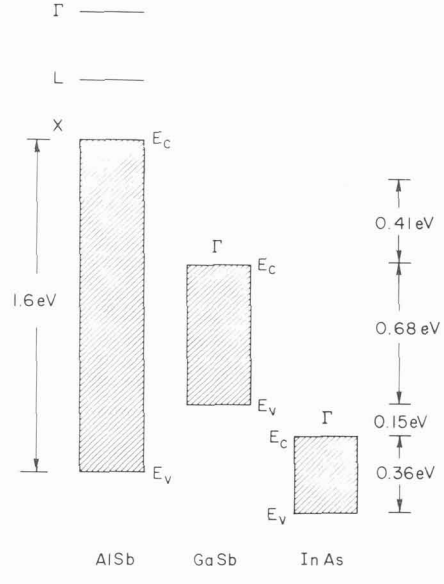

Fig. 18 Estimated bandedge energies of AlSb relative to those of GaSb and InAs. Their energy gaps are indicated by the hatched area.

all lines converge to -38±2 meV at zero magnetic field. We interpret such absorption as being due to interband transitions from H_1 to E_1 Landau levels illustrated in the inset of Fig. 16, where H_1 and E_1 are the ground subbands for heavy holes and electrons, respectively. If these transitions are assumed to occur at a selection rule, $\Delta N=0$, the converged value should correspond to the negative energy gap of the semimetallic superlattice, E_1- H_1. A similar experiment for the 200-100Å sample yielded $E_1 - H_1 = 61 \pm 4$ meV. These values are in good agreement with calculated ones.

Figure 17 shows typical transmission signals[63] as a function of magnetic field for the 1000-1000Å sample which can be considered as a series of isolated heterojunctions. The most pronounced minima are attributed to cyclotron transitions of electrons, which split and become resolvable at high fields. The minima noted CR_h, which are broad and less pronounced in intensity, are believed to be associated with cyclotron transitions of holes. All other features are assigned to interband transitions. The observation of two cyclotron masses appears to manifest the multiple subband structure, as shown in the bottom of Fig. 15, where each subband has its own effective mass.

v) Polytype Superlattices

The superlattice studies in the past were limited to systems involving two host semiconductors or their pseudobinary alloys. We are now considering the introduction of a third constituent such as AlSb in the present InAs-GaSb system,[64] which provides an additional degree of freedom.

The lattice constant of AlSb (6.136Å) is compatible with those of GaSb (6.095Å) and InAs (6.058Å) for heteroepitaxy. Possible bandedge energies of AlSb relative to those of GaSb are illustrated in Fig. 18. If, indeed, the relatively wide energy-gap of AlSb (1.6eV) covers the whole range of the GaSb energy-gap and a part of the InAs energy-gap, AlSb layers serve as potential barriers for electrons as well as holes in superlattices and heterostructures. It should be realized that these three semiconductors, closely matching in lattice constant, yet significantly differing in band parameters, represent a rather unique combination among III-V compound semiconductors.

This triple-constituent system (type III) leads to a new concept of man-made polytype superlattices, ABCABC, ABAC, ACBC, etc., which can never be achieved with the dual-constituent system, as shown in Fig. 19, where A: AlSb, B: GaSb, C: InAs. Since the AlSb layers are expected to be potential barriers, the number of electrons and holes in the structure will be changed by applied electric fields. Thus, this system appears to offer an electrically-controllable medium.

Takaoka et al.[65] studied transport properties of GaSb-AlSb-InAs multiheterojunctions, one of the basic elements in the proposed superlattice. Such structures were prepared by successive MBE growths on p-type GaSb substrates with (100) surface orientation at temperatures: 500C for GaSb, 450-500C for AlSb and 450C for InAs.[66] Heteroepitaxy between GaSb and AlSb with a lattice mismatch of 0.66% appears to proceed smoothly, whereas that between InAs and AlSb with a lattice mismatch of 1.26% indicates a sign of some departure from the ideal case in the observation of streaking RHEED patterns. It is known that the small lattice mismatch is likely accommodated by relaxation involving interfacial atoms, as having been seen in the case of the InAs-GaSb superlattice,[67]

The formation of a GaSb-AlSb superlattice was confirmed metallurgically from x-ray diffraction and optically from electroreflectance and photoluminescence measurements.[68] The luminescence spectra exhibited emission peaks associated with interband transitions between quantum states as well as acceptor impurities. Voisin et al.[69] measured optical transmission near the band gap in a series of GaSb-AlSb superlattices, of which the spectra showed a staircase-like structure characteristic of the two-dimensional electron system. The absorption steps were attributed to transitions between the valence and conduction subbands in the GaSb quantum wells. The energy of the absorption edge, however, was found to be smaller than expected, which was interpreted as a result of the strain effect. Incidentally, photoluminescence from GaSb-AlSb superlattices at 300K was previously studied by Naganuma et al.[70]

vi) InAs Quantum Wells

InAs quantum wells have been investigated with MBE-grown heterostructures GaSb-InAs-GaSb and AlSb-InAs-AlSb, as shown in Fig. 20. Bastard et al.[71] performed self-consistent calculations for the electronic properties of GaSb-InAs-GaSb heterostructures including the effect of high magnetic fields, predicting the existence of a semiconductor-to-semimetal transition when the InAs thickness exceeds a threshold, as a result of electron transfer from GaSb, similar to the situation of the InAs-GaSb superlattice. This was experimental-

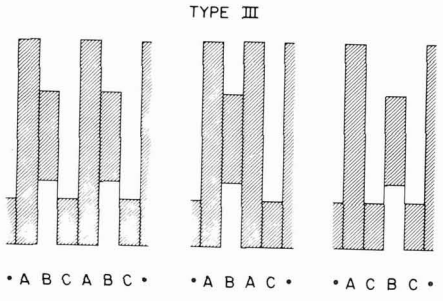

Fig. 19 Potential-energy profiles for polytype (type III) superlattices.

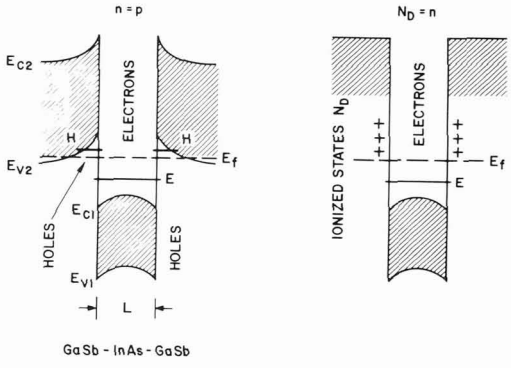

Fig. 20 Energy-band diagrams of InAs quantum wells. The left diagram is for a GaSb-InAs-GaAs heterostructure, whereas the right may be applied to an AlSb-InAs-GaAs heterostructure.

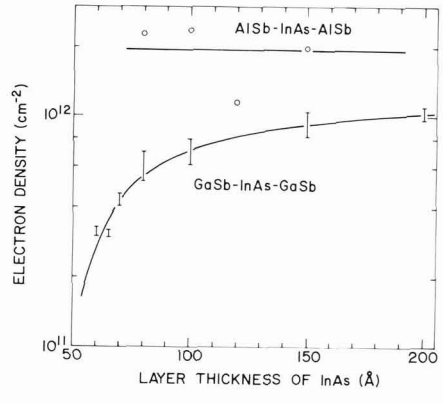

Fig. 21 Electron density at 77K versus InAs layer thickness in AlSb-InAs-AlSb and GaSb-InAs-GaSb heterostructures.

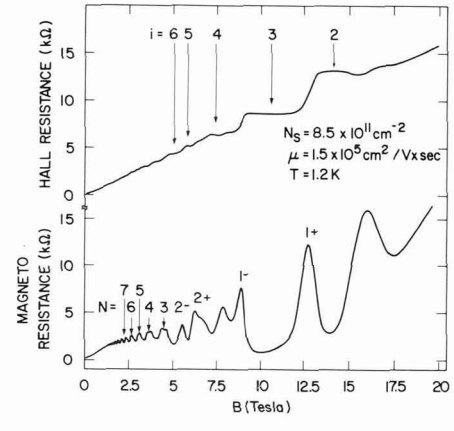

Fig. 22 Magnetoresistance and Hall resistance at 1.2K versus magnetic field for sample 252 (InAs layer thickness of 200Å) with a carrier density of 8.5 x $10^{11} cm^{-2}$ and a mobility of 1.5 x $10^5 cm^2/Vsec$. The arrows in Hall resistance indicate a full Landau level occupation corresponding to i levels.

ly verified by Chang et al.[72] Figure 21 shows the electron densities as a function of the InAs layer thickness, obtained from Hall measurements. In the case of GaSb-InAs-GaSb, where a single quantum well of electrons are sandwiched between two quantum wells of holes, the electron density increases as the InAs layer widens, allowing a larger number of electrons to be transferred. The mobility enhancement with increase in the thickness may be interpreted on the basis of an increase in the carrier screening effect, as well as a reduction in electron-hole scattering.

In the case of AlSb-InAs-AlSb, however, the electron density in the range of $1 \sim 2 \times 10^{12}cm^{-2}$ is unreasonably high and more or less independent on the layer thickness. Although the mobility enhancement with increase in the layer thickness is seen, it reaches a saturation value about a factor of ten lower than that in GaSb confining layers. These results lead us to assume the presence of a large number of positive charge or donor-like states in the vicinity of the interface, as illustrated in the right of Fig. 20. These states not only provide electrons but also may act as scattering centers, resulting in high electron densities and low mobilities. Nevertheless, magneto-transport measurements have demonstrated the presence of two-dimensional electrons, showing pronounced oscillations at 4.2K.

Mendez et al.[73] studied the quantized Hall effect for two-dimensional carriers confined in GaSb-InAs-GaSb heterostructures. In contrast to previously investigated systems such as GaAs-GaAlAs, the present heterostructures offer a new medium where a two-dimensional electron gas formed in InAs coexists with a two-dimensional hole gas, of the same density, formed in the GaSb side: The intrinsic nature of the bandedge relationship determined the carrier density. Figure 22 shows magnetoresistance and Hall resistance as a function of magnetic field for a high-mobility sample, developing well-defined Hall-resistance plateaus in good agreement with the theoretical value (h/ie^2). The magnetoresistance exhibits a typical oscillatory behavior, corresponding to the crossing of the Landau levels (N=1, 2, 3...) with the Fermi level where, at moderate fields, it is noticeable that the levels are spin-split, as indicated by the $\pm$ signs in Fig. 22. In addition to these regular characteristics, extra features are revealed, as seen at 8 and 16T, which could result from the presence of holes and, particularly, electron-hole interaction of which the nature is not well understood at the present time.

4) Other Superlattice Structures

i) Other Semiconductor Systems

A variety of semiconductor pairs have been exploited to synthesize superlattices and heterostructures. Compared to GaAs-GaAlAs and InAs-GaSb, however, other superlattice studies are still in their infancy; in many cases, experimental results do not show as high a degree of sophistication as we have seen in the GaAs-GaAlAs system, partly because of their inferior structural quality, even though a number of intriguing proposals were made on the theoretical basis.

Nevertheless, high-quality interfaces can be obtained with InP-based lattice-matched systems. Rezek et al.[74] succeeded with a Double Heterojunction (DH) laser using InP-InGaPAs multiple thin layers. More recently, Brummell et al.[75] and Voos[76] reported magnetotransport as well as other important experiments in MOCVD-grown InP-InGaAs superlattices and heterojunctions.

Osbourn[77] proposed strained-layer superlattices from a variety of material systems including the alloys of GaAs-GaP and GaAs-InAs on a premise that lattice-mismatched heterostructures can be grown with essentially no misfit defect generation, if the layers are sufficiently thin, because the mismatch is accommodated by uniform lattice strain.[78] The GaAs-GaAsP system, which was theoretically analyzed in this proposal,[77] actually was the first superlattice experimentally investigated.[7] Ludowise et al.[79] observed stimulated emission in strained-layer GaAs-$GaAs_{0.75}P_{0.25}$ superlattices with photoexcitation. Osbourn et al.[80] (Gourley et al.[81]) claimed the growth of a direct-gap (2.03eV), strained-layer superlattice with indirect-gap hosts, GaP and $GaAs_{0.4}P_{0.6}$, due to Brillouin-zone folding. Camras et al.[82] presented data showing that Zn diffused into a strained layer GaP-$GaAs_{0.4}P_{0.6}$ superlattice enhanced the interdiffusion of As and P at the interfaces, resulting in a disordered $GaAs_{0.2}P_{0.8}$ bulk crystal. Fritz et al.[83] reported doping and transport properties of a GaAs-$Ga_{0.8}In_{0.2}As$ strained-layer superlattice. Kim et al.[84] theoretically treated GaP-AlP superlattices with varying thickness, showing that the superlattices exhibit a direct-gap behavior.

The Ge-GaAs system is perhaps the oldest example of heteroepitaxy[85] with nearly perfect lattice-matching. Recently, the electronic structure at this interface, which involves both polar and nonpolar faces, has drawn considerable attention for theoretical considerations: Baraff et al.,[86] Pickett et al.,[87] Harrison et al.,[88] and Pollmann et al.[89] (including Ge-ZnSe(100) interfaces). The heteroepitaxial growth of a compound semicon-

ductor on an elemental semiconductor, however, turns out to present unsurmountable technical problems such as formation of two possible sublattices, charge neutrality, diffusion, etc. Such problems apparently prevent the achievement of the structural perfection. Petroff et al.[90] and Chang et al.[91] reported the MBE growth of Ge-$Ga_{1-x}Al_xAs$ (ultra-thin layer) and Ge-GaAs superlattices, respectively, together with the results of their metallurgical analyses. Bauer et al.[92] studied surface processes controlling Ge-GaAs(100) heterojunction formation. Madhukar et al.[93] calculated the electronic structure of Si-GaP(100) interface and superlattice.

Kasper et al.[94] reported the growth of a $Si-S_{0.85}$ $Ge_{0.15}$ superlattice by UHV epitaxy with its metallurgical characterization including dislocations. Manasevit et al.[95] observed enhanced Hall mobilities in (100)-oriented, n-type $Si-Si_{1-x}Ge_x$ multilayer films.

Schulman et al.[96] theoretically treated a CdTe-HgTe superlattice, showing that its band gap is adjustable from 0 to 1.6eV depending on the thickness of the CdTe and HeTe layers. The usefulness of this superlattice for infrared optoelectric devices was suggested. Faurie et al.[97] reported the MBE growth of CdTe-HgTe superlattices which were characterized by Auger electron spectroscopy and ion microprobe profiling measurements.

Kinoshita et al.[98] successfully prepared PbTe-$Pb_{0.8}Sn_{0.2}Te$ superlattices by the hot wall technique on BaF_2 substrates, which were profiled by sputtering-Auger electron spectroscopy in conjunction with the investigation of the interdiffusion of Pb and Sn. More recently, Shubnikov-de Haas oscillations[99] were observed for two-dimensional electrons with a mobility of 1.9 x $10^5 cm^2/Vsec$ in modulation Bi-doped superlattices. Partin[100] reported the MBE growth of PbTe-$Pb_{0.97}Ge_{0.03}Te$ superlattices with their metallurgical characterization.

ii) Ultra-Thin Layer Superlattices

Gossard et al.[101] reported the achievement of an ultra-thin layer superlattice by alternate monolayer depositions of GaAs and AlAs. Transmission electron microscopy showed such a MBE-grown structure to be perfectly epitaxial with layered composition modulation of the expected periodicity, although dark-field transmission electron micrographs indicated the presence of disordered regions along with ordered monolayer domains. The electronic properties were studied by optical absorption and luminescence. Petroff et al.[90] studied the MBE growth of Ge-$Ga_{1-x}Al_xAs$ ultra-thin layer superlattice, as previously mentioned. They also attempted alternate monolayer depositions with two components with a sizable lattice mismatch such as a pair of GaAs and InAs.

iii) Doping superlattices (n-i-p-i)

Döhler[102] and Ploog et al.[103] pursued a doping superlattice which was included in the original proposal,[1,2] as shown in the top of Fig. 3. The periodic rise and fall of the conduction and valence bands is caused by a periodic variation of impurity concentration, where electrons are attracted to minima in the conduction band while holes are attracted to maxima in the valence band. If this superlattice is illuminated, extra electrons and holes are created, which are to be spatially separated because of the above-mentioned reason. Therefore, they can have anomalously long lifetimes. An interesting consequence of this fact is that the amplitude of the periodic potential is reduced by the extra carrier, leading to a crystal which has a variable energy gap. Döhler et al.[104] indeed observed that the photon energies in luminescence, which represent the band gap, were varied from 1.3eV to 1.53eV by the laser excitation intensity. In addition, Raman experiments provided an evidence of electronic subbands in purely space-charge-induced quantum wells. The doping superlattice used here was grown by MBE, which consists of twenty n- and p-doped GaAs layers with equal doping concentration of $10^{18} cm^{-3}$. The individual layer thickness is 400Å.

IV. SUMMARY

It has been more than a decade since Esaki and Tsu, in their original proposal[2] stated, "The study of superlattices and observation of quantum mechanical effects on a new physical scale may provide a valuable area of investigation in the field of semiconductor physics." In the meantime, the evolution of MBE as a technique for the growth of ultra-thin layers of high-quality semiconductors allowed access to such a new quantum regime. Indeed, in recent years, considerable attention has been given to the engineering of artificial structures such as superlattices, quantum wells and other multiheterojunctions. Obviously, the intriguing physics, particularly regarding the electron gas system of the reduced dimensionality involved in such structures, has provided fuel for this advancement. The described InAs-GaSb research is one example which elucidates the salient features involved in synthesized superlattices. In that case, important electronic

parameters such as energy gaps (including negative gaps) can be engineered by introducing made-to-order superlattice potentials: some of its unique properties may not even exist in any "natural" crystal.

We believe that efforts in this direction apparently have opened up a new area of interdisciplinary investigations in the fields of materials science and device physics. A variety of materials, including III-V, II-VI, IV-VI compounds, as well as elemental semiconductors, have been exploited for the synthesis of superlattices. In fact, the progress in the semiconductor superlattice has inspired investigations on metallic superlattices[105] and even amorphous multilayered structures.[106] In the area of semiconductor devices, ideas originating from the superlattice have found their applications in heterojunction field-effect transistors (HEMT or TEGFET), quantum-well lasers and novel avalanche photodiodes. Superlattice is now one of the most lively areas, where new results are flowing in with enthusiasm. I hope this review, which cannot possibly cover every landmark, provides a little flavor to this excitement.

ACKNOWLEDGMENTS

Our investigation on superlattices was sponsored in part by the ARO.

REFERENCES

1. ESAKI, L. and TSU, R., IBM Research Note RC-2418 (1969).
2. ESAKI, L. and TSU, R., IBM J. Res. Develop. 14 (1970) 61.
3. BOHM, D. *Quantum Theory* (Prentice Hall, Englewood Cliffs, N.J. 1951) 283.
4. ESAKI, L. *Les Prix Nobel en 1973*, Imprimerie Royale P. A. Norstedt & Söner , Stockholm 1974, p. 66; Science 183 (1974) 1149.
5. KRONIG, R. de L. and PENNEY, W. J. Proc. Roy. Soc. A130 (1930) 499.
6. GNUTZMAN, U. and CLAUSEKER, K. Appl. Phys. 3 (1974) 9.
7. ESAKI, L., CHANG, L.L. and TSU, R., Proceedings 12th International Conference on Low Temperature Physics, Kyoto, Japan, September 1970. (Keigaku Publishing Co., Tokyo, Japan) 551.
8. CHANG, L. L., ESAKI, L., HOWARD, W. E. and LUDEKE, R. J. Vac. Sci. Technol. 10, (1973) 11; CHANG, L. L., ESAKI, L., HOWARD, W. E., LUDEKE, R. and SCHUL, G., J. Vac. Sci. Technol. 10 (1973) 655.
9. ESAKI, L., CHANG, L. L., HOWARD, W. E., and RIDEOUT, V. L. Proceedings of the 11th International Conference on the Physics of Semiconductors, Warsaw, Poland, 1972, edited by the Polish Academy of Sciences (PWN-Polish Scientific Publishers, Warsaw, Poland, 1972) 431.
10. LUDEKE, R., ESAKI, L. and CHANG, L. L., Appl. Phys. Lett. 24 (1974) 417.
11. TSU, R., and ESAKI, L., Appl. Phys. Lett. 22 (1973) 562.
12. CHANG, L. L., ESAKI, L. and TSU, R., Appl. Phys. Lett. 24 (1974) 593.
13. ESAKI, L. and CHANG, L. L., Phys. Rev. Lett. 33 (1974) 495.
14. SEGMÜLLER, A., KRISHNA, P. and ESAKI, L., J. Appl. Cryst. 10 (1977) 1.
15. WEISBUCH, C., DINGLE, R., GOSSARD, A. C., and WIEGMANN, W., *Solid State Commun.* 38 (1981) 709.
16. See, for example, COHEN, M. L., Advances in Electronics and Electron Physics, Vol. 51, 1, Academic Press, 1980.
17. HARRISON, Walter A., J. Vac. Sci. Technol. 14 (1977) 1016.
18. FRENSLEY, W. R. and KROEMER, H., Phys. Rev. B16 (1977) 2642.
19. BASTARD, G., Phys. Rev.B, 24 (1981) 5693.
20. WHITE, S. R. and SHAM, L. J. Phys. Rev. Lett. 47 (1981) 879.
21. DINGLE, R., WIEGMANN, W. and C. H. Henry, Phys. Rev. Lett. 33, (1974) 827.
22. DINGLE, R., GOSSARD, A. C., and WIEGMANN, W., Phys. Rev. Lett. 34 (1975) 1327.
23. Van Der ZIEL, J. P., DINGLE, R., MILLER, R. C., WIEGMANN, W. and NORDLAND JR., W. A., Appl. Phys. Lett. 26 (1975) 463.
24. TSANG, W. T., Appl. Phys. Lett. 39 (1981) 786.
25. TSU, R., CHANG, L. L., SAI-HALASZ, G. A. and ESAKI, L., Phys. Rev. Lett. 34 (1975) 1509.
26. MENDEZ, E. E., BASTARD, G., CHANG, L. L., ESAKI, L., MORKOC, H. and FISCHER, R., Phy. Rev. B26 (1982) 7101 and Physica 117B & 118B, (1983) 711.
27. MANUEL, P., SAI-HALASZ, G. A., CHANG, L. L., CHANG, C-A. and L. Esaki, Phys. Rev. Lett. 25 (1976) 1701.
28. BURSTEIN, E., PINCZUK, A. and BUCHNER, S., Physics of Semiconductors 1968, Institute of Physics Conference Series 43, London, 1979, 1231.
29. ABSTREITER, G.and PLOOG, K., Phys. Rev. Lett. 42 (1979) 1308.

30. PINCZUK. A., STÖRMER, H. L., DINGLE, R., WORLOCK, J. M., WIEGMANN, W. and GOSSARD, A. C., Solid State Commun. 32 (1979) 1001.
31. COLVARD, C., MERLIN, R., KLEIN, M. V., and GOSSARD, A. C. Phys. Rev. Lett. 45 (1980) 298.
32. CHANG, L. L., SAKAKI, H., CHANG, C. A.,and ESAKI, L., Phys. Rev. Lett. 38 (1977) 1489.
33. TSUI, D. C. and ENGLERT, Th. Phys. Rev. Lett. 44 (1980) 341.
34. DINGLE, R., STÖRMER, L., GOSSARD, A. C., and WIEGMANN, W., Appl. Phys. Lett. 33 (1978) 665.
35. MIMURA, R., HIYAMIZU, S., FUJII, T. and NANBU, K., Jpn. J. Appl. Phys. 19 (1980) L225.
36. DELAGEBEAUDEUF, D., DELESCLUSE, P., ETIENNE, P., LAVIRON, M., CHAPLART, J., and LINH, N. T., Electron. Lett. 16 (1980) 667.
37. KLITZING, K. v., DORDA, G., and PEPPER, M. ,Phys. Rev. Lett. 45 (1980) 494.
38. TSUI, D. C., and GOSSARD, A. C. Appl. Phys. Lett. 38, (1981) 550.
39. TSUI, D. C., GOSSARD, A. C., FIELD, B. F., CAGE, M. E. and DZIUBA, R. F., Phys. Rev. Lett. 48, (1982) 3.
40. TSUI, D. C., STÖRMER, H. L., and GOSSARD, A. C., Phys. Rev. Lett. 48, (1982) 1559.
41. MENDEZ, E. E., HEIBLUM, M., CHANG, L. L. and ESAKI, L., to be published.
42. LAUGHLIN, R. B., Phys. Rev. Lett. 50 (1983) 1395.
43. STÖRMER, H. L., CHANG, A., and TSUI, D. C., Phys. Rev. Lett. 50 (1983) 1953.
44. BASTARD, G., Phys. Rev. B, 24, (1981) 4714; Surf. Sci. 113 (1982) 165.
45. MILLER, R. C., GOSSARD, A. C., TSANG, W. T., and MUNTEANU, O., Solid State Commun. 43 (1982) 519; MILLER, R. C., GOSSARD, A. C., TSANG, W. T., and MUNTEANU, O., Phys. Rev. B 25 (1982) 3871.
46. BASTARD, G., MENDEZ, E. E., CHANG, L. L., and ESAKI, L., Phys. Rev. B 26 (1982) 1974.
47. GREENE, Ronald L. and BAJAJ, K. K., Solid State Commun. 45 (1983) 831; GREENE, Ronald L. and BAJAJ, K. K., Solid State Commun. 45 (1983) 825.
48. CHIN, R., HOLONYAK, N., STILLMAN, Jun. G. E. Electronics Letters, 16 (1980) 467.
49. CAPASSO F., TSANG, W. T., HUTCHINSON, A. L., and WILLIAMS, G. F., Appl. Phys. Lett. 40 (1982) 38.
50. CAPASSO, Federico, J. Vac. Sci. Technol. B 1 (1983) 457.
51. TANOUE, T. and SAKAKI, H., Appl. Phys. Lett. 41 (1982) 67.
52. SAKAKI, Hiroyuki, Jpn. J. Appl. Phys. 19 (1980) L735.
53. PETROFF, P. M., GOSSARD A. C., LOGAN, R. A., and WIEGMANN, W., Appl. Phys. Lett. 41 (1982) 635.
54. SAKAKI, H., CHANG, L. L., LUDEKE, R., CHANG, C-A., SAI-HALASZ, G. and ESKAI, L., Appl. Phys. Lett. 31 (1977) 211.
55. SAI-HALASZ, G. A., TSU, R., and ESAKI, L. Appl. Phys. Lett. 30 (1977) 651.
56. SAI-HALASZ, G. A., ESAKI, L., and HARRISON W. A., Phys. Rev. B18 (1978) 2812.
57. SAI-HAlASZ, G. A., CHANG, L. L., WELTER, J-M., CHANG, C-A. and ESAKI, L., Solid State Commun. 25 (1978) 935.
58. VOISIN, P., BASTARD, G., GONCALVES DA SILVA , C.E.T., VOOS, M., CHANG, L. L., and ESAKI, L, Solid State Commun. 39 (1981) 79.
59. CHANG, L. L., KAWAI, N. J., SAI-HALASZ, G. A., LUDEKE, R. and ESAKI, L., Appl. Phys. Lett. 35 (1979) 939.
60. CHANG, L. L., KAWAI, N. J., MENDEZ, E. E., CHANG, C-A., and ESAKI, L., Appl. Phys. Lett. 38 (1981) 30.
61. GULDNER, Y., VIEREN, J., VOISIN, P., VOOS, M., CHANG L. L., and ESAKI, L., Phys. Rev. Lett. 45 (1980) 1719.
62. MAAN, J. C.,GULDNER, Y., VIEREN, J. P., VOISIN, P., VOOS, M., CHANG, L. L. and ESAKI, L. Solid State Commun. 39 (1981) 683.
63. GULDNER, Y., VIEREN, J. P. Vieren, VOISIN, P., VOOS, M., MAAN, J. C., CHANG, L. L. and ESAKI, L., Solid State Commun. 41 (1982) 755.
64. ESAKI, L., CHANG, L. L., and MENDEZ, E. E., Jpn. J. Appl. Phys. 20 (1981) L529.
65. TAKAOKA, H., CHANG, C-A, MENDEZ, E. E., CHANG, L. L. and ESAKI, L., Physica 117B & 118B (1983) 741. on the Physics of Semiconductors, Montpellier, France, 1982.
66. CHANG, C-A., TAKAOKA, H., CHANG,L. L., and ESAKI, L., Appl. Phys. Lett. 40 1982) 983.
67. SARIS, F. W., CHU, W. K., CHANG, C-A, LUDEKE, R. and ESAKI, L., Appl. Phys. Lett 37 931 (1980).
68. MENDEZ, E. E., CHANG, C.-A., TAKAOKA, H., CHANG, L. L. and ESAKI, L., J. Vac. Sci. Technol. B1 (1983) 152.
69. VOISIN, P., BASTARD, G., and VOOS, M., J. Vac. Sci. Technol. B1 (1983) 409.

70. NAGANUMA, M., SUZUKI, Y., and OKAMOTO, H., in Proc. Int. Symp. GaAs and Related Compounds, ed. by T. Sugano (Institute of Physics, University of Reading, Berkshire, 1981) 125.
71. BASTARD, G., MENDEZ, E. E., CHANG, L. L., and ESAKI, L., J. Vac. Sci. Technol. 21 (1982) 531.
72. CHANG, C. A., MENDEZ, E. E., CHANG, L. L., and ESAKI, L., to be published.
73. MENDEZ, E. E., CHANG, L. L., CHANG, C-A., ALEXANDER, L. F. and ESAKI, L., to be published.
74. REZEK, E. A., HOLONYAK, N. Jr., VOJAK, B. A., STILLMAN, G. E., ROSSI, J. A., KEUNE, D. L., and FAIRING, J. D., Appl. Phys. Lett. 31 (1977) 288.
75. BRUMMELL, M. A., NICHOLAS, R. J., PORTAL J. C., RAZEGHI, M., and POISSON, M. A., Physica 117B & 118B (1983) 753.
76. VOOS, M., J. Vac. Sci. Technol. B1 (1983) 404.
77. OSBOURN, G. C., J. Appl. Phys. 53 (1982) 1586.
78. VAN DER MERWE, J. Appl. Phys., 34 (1963) 117.
79. LUDOWISE,M. J., DIETZE, W. T., LEWIS, C. R., HOLONYAK, N. Jr., HESS, K., CAMRAS, M. D., and NIXON, M. A., Appl. Phys. Lett. 42 (1983) 257. 80.OSBOURN, G. C., BIEFELD, R. M. and GOURLEY, P. L. Appl. Phys. Lett. 40, (1982) 173.
81. GOURLEY, P. L., and BIEFELD, R. M., J. Vac. Sci. Technol. 21 (1982) 473.
82. CAMRAS, M. D., HOLONYAK, N. Jr., HESS, K., LUDOWISE, M. J., DIETZE, W. T., and LEWIS, C. R., Appl. Phys. Lett. 42 (1983) 185.
83. FRITZ, I. J. DAWSON, L. R. and ZIPPERIAN, T. E., J. Vac. Sci. Technol. B1 (1983) 387.
84. KIM, J. Y. and MADHUKAR, A., J. Vac. Sci. Technol. 21 (1982) 526.
85. ANDERSON, R. L., IBM J. Res. Develop. 4 (1960) 283; ESAKI, L., HOWARD, W. E., and HEER, J., Appl. Phys. Lett. 4 (1964) 3.
86. BARAFF, G. A., APPELBAUM, Joel A., and HAMANN, D. R., J. Vac. Sci. Technol. 14 (1977) 999.
87. PICKETT, W. E., LOUIS, S. G., and COHEN, M. L., Phys. Rev. Lett. 39 (1977) 109.
88. HARRISON, W. A., KRAUT, E., WALDROP, J. R., and GRANT, R. W., Phys. Rev. B18 (1978) 4402.
89. POLLMANN, J. and PANTELIDES, S. T., Phys. Rev. B21 (1980) 709.
90. PETROFF, P. M., GOSSARD, A. C., SAVAGE, A., and WIEGMANN, W., J. Cryst. Growth 46 (1979) 172.
91. CHANG, Chin-An, SEGMÜLLER, A., CHANG, L. L. and L. Esaki, Appl. Phys. Lett. 38 (1981) 912.
92. BAUER Robert S. and MIKKELSEN, J. C., Jr., J. Vac. Sci. Technol. 21 (1982) 491.
93. MADHUKAR, A. and DELGADO., Solid State Commun. 37 (1981) 199.
94. KASPER, E., HERZOG, H.J. and KIBELL, H., Appl. Phys. 8 (1975) 199.
95. MANASEVIT, H. M., GERGIS, I. S., and JONES, A. B., Appl. Phys. Lett. 41 (1982) 464.
96. SCHULMAN, J. N., and McGILL, T. C., Appl. Phys. Lett. 34 (1979) 883.
97. FAURIE,J. P., MILLION, A., and PIAGUET, J., Appl. Phys. Lett. 41 (1982) 713.
98. KONSHITA, H. and FUJIYASU, H., J. Appl. Phys. 51 (1980) 5845.
99. KINOSHITA, H., TAKAOKA, S., MURASE K. and FUJIYASU, H., Proc. of 2nd International Symposium on Molecular Beam Epitaxy and Related Clean Surface Techniques, Tokyo, Japan, p. 61.
100. PARTIN, D. C., J. Vac. Sci. Technol. 21 (1982) 1.
101. GOSSARD, A. C., PETROFF, P. M., WEIGMANN, W., DINGLE, R., and SAVAGE, A., Appl. Phys. Lett. 29 (1976) 323.
102. DÖHLER, G. H., Phys. Status Solidi (b) 52 (1972) 79 and 533.
103. PLOOG, K., FISCHER, A., DÖHLER, G. H. and KÜNZEL, H., in *Gallium Arsenide and Related Compounds 1980*, Institute of Physics Conference Series No. 56, edited by H. W. Thim (Institute of Physics, London, 1981), 721.
104. DÖHLER, G. H., KÜNZEL,H., OLEGO, D., PLOOG, K., RUDEN, P., STOLZ, H. J. and ABSTREITER, G., Phys. Rev. Lett. 47 (1981) 864.
105. SCHULLER, I. K., and FALCO, C. M., Surf. Sci. 113 (1982) 443.
106. OGINO, I., TAKEDA, A. and MIZUSHIMA, Y., Proceedings of the Second International Symposium on MBE and Related Clean Surface Techniques, Tokyo, Japan 1982, 65.